

Influence of Particle Size Distribution on Random Close Packing

Kenneth W. Desmond and Eric R. Weeks

Department of Physics, Emory University, Atlanta, Georgia 30322, USA

(Dated: June 18, 2022)

The densest amorphous packing of rigid particles is known as random close packing. It has long been appreciated that higher densities are achieved by using collections of particles with a variety of sizes. The variety of sizes is often quantified by the polydispersity of the particle size distribution: the standard deviation of the radius divided by the mean radius. Several prior studies quantified the increase of the packing density as a function of polydispersity. Of course, a particle size distribution is also characterized by its skewness, kurtosis, and higher moments, but the influence of these parameters has not been carefully quantified before. In this work, we numerically generate many packings with different particle radii distributions, varying polydispersity and skewness independently of one another. We find two significant results. First, the skewness can have a significant effect on the packing density and in some cases can have a larger effect than polydispersity. Second, the packing fraction is relatively insensitive to the value of the kurtosis. We present a simple empirical formula for the value of the random close packing density as a function of polydispersity and skewness.

I. INTRODUCTION

Understanding various aspects of random close packing (*rcp*) has great scientific and industrial importance [1] as it has been linked to a wide range of problems such as the structure of living cells [2], liquids [3, 4], granular media [5–8], emulsions [9], glasses [10], amorphous solids [11], jamming [12, 13], and the processing of ceramic materials [14]. Random close packing is typically defined as a collection of particles packed into the densest possible configuration, although more rigorous definitions are available [15]. Experiments have found that the densest random packing of monodisperse spheres typically occurs close to $\phi_{0,rcp} \sim 0.64$ [4], where the density ϕ (or packing fraction) is defined as the ratio of the total volume occupied by spheres to the volume of the container.

Formally, a packing consists of particles with a distribution in radii $P(R)$. The polydispersity is defined as $\delta = \sqrt{\langle \Delta R^2 \rangle} / \langle R \rangle$. Here, $\Delta R = R - \langle R \rangle$ and the moments of R (and ΔR) are defined as $\langle R^n \rangle = \int R^n P(R) dR$ (and $\langle \Delta R^n \rangle = \int \Delta R^n P(R) dR$). It has long been appreciated that packings of spheres can have other *rcp* densities when $\delta > 0$ [16–21]. Prior experiments [22–26] and simulations [27–31] have nicely shown that as the polydispersity increases, the particles pack to higher volume fractions because the smaller particles pack more efficiently by either layering against larger particles or by fitting into the voids created between neighboring large particles [23, 32–34]. In practice, depending on the degree of the polydispersity, the packing fraction can increase from 0.64 for monodisperse packings to nearly ~ 0.75 for packings with 0.65 polydispersity [23]. For the extreme case of two different particle sizes with a size ratio approaching infinity, the voids between the large particles can be packed randomly with small particles and so ϕ can be as large as $\phi_{0,rcp} + (1 - \phi_{0,rcp})\phi_{0,rcp} \approx 0.88$ [23, 35].

While it is intuitive that the polydispersity can affect ϕ_{rcp} , it is also reasonable that the shape, not just the spread, of the distribution $P(R)$ may also influence

ϕ_{rcp} [1, 23]. For instance, an infinite number of distributions can have the same value of δ but yet differ in their form. One can characterize the shape using the skewness $S = \langle \Delta R^3 \rangle / \langle \Delta R^2 \rangle^{3/2}$, kurtosis $K = \langle \Delta R^4 \rangle / \langle \Delta R^2 \rangle^2$, and higher moments. There have been prior studies that have investigated the influence of distribution shape on the density of tightly packed particles [14, 23, 34, 36–40]. Similar to the studies on polydispersity, they find that the shape of the particle distribution can have a profound influence on the packing density. However, these prior studies either did not independently vary δ and S but rather conflated the influences of both, or else used other metrics besides δ and S to quantify $P(R)$. Of the prior studies, Tickell *et al.* [41] is the only one to report on the effects of skewness and kurtosis for experiments carried out with sand, finding that over a narrow range in skewness the packing density can increase by 0.04 with no dependence on kurtosis. However, they did not control for polydispersity, leaving it unclear the relative importance of polydispersity and skewness. The key unanswered question by the prior work is how the skewness of a distribution influences ϕ_{rcp} , and large this effect is relative to the effects of polydispersity.

To study the influence of skewness on ϕ_{rcp} , we generate random close packings numerically, and control for polydispersity and skewness independently to address how dominant each term is in determining ϕ_{rcp} . Our method for generating these packings was previously developed in Ref. [42]. Briefly, infinitesimal particles are placed randomly in a periodic container, gradually expanded, and moved at each step to prevent particles from overlapping. At the beginning of the simulation, particles are assigned radii with a specific distribution and as the particles expand they do so by a multiplicative factor such that the shape of the radii distribution is fixed. The value of ϕ_{rcp} is known to be sensitive to protocol [43, 44], and it is not known if this algorithm or any other algorithm produces rigorously defined random close packed states [15, 42, 45, 46]. Our goal is not to determine the precise value of ϕ_{rcp} for a given $P(R)$, but rather

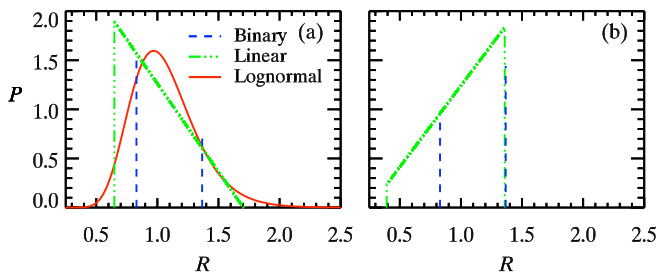


FIG. 1. (Color online). (a) Examples of three different particle radii distributions with the same polydispersity of 0.25 and nearly the same skewness. The binary distribution has $S = 0.78$, the linear distribution has $S = 0.56$, and the lognormal distribution has $S = 0.78$. (b) Examples of two different particle radii distributions with the same polydispersity of 0.25 and negative skewness $S = -0.5$.

to empirically understand the trend in ϕ_{rcp} with polydispersity and skewness. Nonetheless, we note that our algorithm when applied to a monodisperse packing gives $\phi_{0,rcp} \sim 0.64$, close to the experimentally found value and in agreement with prior simulation work.

To efficiently determine ϕ_{rcp} for a chosen particle size distribution, we exploit the known finite size dependence $\phi_{rcp}(h) = \phi_{rcp}^{\infty} - C/h$, where h is the system size, ϕ_{rcp}^{∞} is the random close packing fraction in the limit $h \rightarrow \infty$, and C is a fitting constant [47]. By generating many packings with different box sizes h , we fit $\phi_{rcp}(h)$ to determine ϕ_{rcp}^{∞} for each distribution. We generate packings with box sizes of $\sim 10, 14, 18$, and 23 mean particle diameters in length to determine ϕ_{rcp}^{∞} . For the rest of the paper, ϕ_{rcp} will be used to indicate ϕ_{rcp}^{∞} .

To control for both δ and S independently, we study packings using four different distributions: binary, linear, gaussian, and lognormal. The binary and linear distributions are determined by two control parameters, allowing for us to control δ and S independently, while the gaussian and lognormal distributions are determined by only one parameter, and therefore δ and S can not be controlled independently. By generating many packings with different δ and S using these four distributions, we can compare the results to see how sensitive ϕ_{rcp} is to polydispersity and skewness, but we can also compare different distributions with the same δ and S to see how sensitive ϕ_{rcp} is to other subtle differences in the distribution shape. For all distributions, we impose $\langle R \rangle = 1$.

More specifically, the binary distribution consists of particles with two distinct radii. The shape of the distribution is determined by the size ratio and number ratio of these two particle types. The linear distribution is a continuous distribution of the form $P(R) = AR + B$, where the distribution in particle size exists over a finite range $a \leq R \leq b$. Our choice of $\langle R \rangle = 1$ and the requirement of normalization ($\int_a^b P(R) dR = 1$) imposes two constraints on the parameters (a, b, A, B). For the two remaining degrees of freedom, we define $\eta = b/a$ and $\rho = P(a)/P(b)$.

We compute S and δ for a grid of η and ρ values, and then interpolate to find the parameters for $P(R)$ for the desired S and δ values, allowing us to vary them systematically. The third distribution is a Gaussian of the form $P(R) = A_G \exp(-(R-1)^2/2\sigma^2)$, where σ is the standard deviation and $A_G = 1/(\sigma\sqrt{2\pi})$. For larger σ , some of the particle radii could be negative, which is unphysical, or very close to zero, which may prevent generating packings within a reasonable timeframe. To avoid these issues, we truncate the Gaussian distribution such that the smallest particle radius is no smaller than 0.1. The Gaussian distribution has a fixed skewness $S = 0$ except for the truncated Gaussians, which have a slight positive skewness. The last distribution we consider is the lognormal distribution $P(R) = A_L \exp(-0.5(\ln R/\sigma + 0.5\sigma)^2)/R$, where $A_L = 1/(\sigma\sqrt{2\pi})$. Similar to the Gaussian distribution, the skewness of the lognormal distribution is not adjustable, but is always positive and becomes larger as σ becomes larger.

In Fig. 1(a), we compare three different distributions with polydispersity $\delta = 0.25$ and nearly the same positive skewness $S \approx 0.75$. We see that the distributions are quite different, in particular in their tails. For example, the linear distribution has many more small particles than the other two distributions. The lognormal distribution has tails that include both smaller and larger particles than the other two distributions. It's not necessarily obvious how the values of ϕ_{rcp} will be ranked for these cases. In Fig. 1(b), we show two different distributions with polydispersity $\delta = 0.25$ and skewness $S \approx -0.5$. As these distributions have negative skewness, both distributions have more larger particles than smaller particles. Once again, it's not necessarily clear how ϕ_{rcp} should differ between the two packings.

After generating nearly 10,000 packings with different particle radii distributions, we plot ϕ_{rcp} as a function of skewness S for all our data in Fig. 2, with the different groups of data (different colors) corresponding to different polydispersity values δ . Each data point in the figure has a one to one correspondence to the distribution type, δ , and S . The symbol or line type of the data indicates the $P(R)$ distribution type. Remarkably, the figure shows that regardless of the type of particle radii distribution, ϕ_{rcp} is nearly the same for the same pairing of polydispersity and skewness. It also shows that ϕ_{rcp} increases with both increasing δ and S . Strikingly, the skewness can have an equally important effect as the polydispersity. For example, for $\delta = 0.40$ and $S = 0$, ϕ_{rcp} is shifted upward by ≈ 0.02 . Fixing that value of δ , changing S to ± 1 shifts ϕ_{rcp} by $\approx \pm 0.02$. For highly polydisperse samples, one cannot accurately know ϕ_{rcp} without also knowing the skewness of the radius distribution. For the binary samples (solid lines in Fig. 2) S can be even larger in magnitude and have an even larger influence on ϕ_{rcp} than δ has.

The increase in ϕ_{rcp} with skewness is not uniform. For negative skewness (more big particles), the polydispersity δ does not seem to influence ϕ_{rcp} as much as when

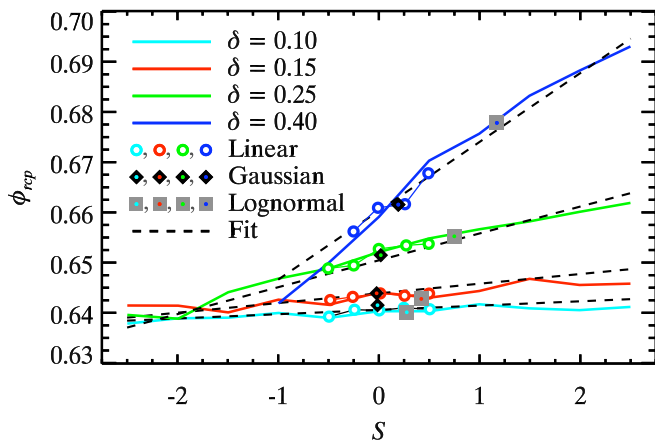


FIG. 2. (Color online). This figure shows how ϕ_{rcp} depends on particle size distribution, polydispersity δ , and skewness S . The solid lines represent ϕ_{rcp} for binary packings and the symbols represent ϕ_{rcp} for packings with either linear, Gaussian, or lognormal particle distributions as indicated by the legend. The colors represent different polydispersities of either 0.1, 0.15, 0.25, or 0.4. The dashed lines are a fit to the data using $\phi_{rcp} = \phi_{rcp}^* + c_1\delta + c_2S\delta^2$, where $\phi_{rcp}^* = 0.634$, $c_1 = 0.0658$, and $c_2 = 0.857$.

the skewness is positive. This is not too surprising since the volume of each particle grows with R^3 . When the total number of bigger particles is greater than the total number of smaller particles (negative skewness), the volume occupied by all the large particles is significantly greater than the volume occupied by all the small particles. In effect, the big particles pack like a low polydispersity sample and occupy the majority of the container, while the small spheres occupy an insignificant portion, and ϕ_{rcp} approaches $\phi_{0,rcp} \approx 0.64$ for a monodisperse sample. For positive skewness (more smaller particles), ϕ_{rcp} has a fairly strong dependence on δ and S , where ϕ_{rcp} increases with increasing number of small particles. The reason for this increase in ϕ_{rcp} is likely due to the small particles fitting into the spaces between larger particles. As discussed in prior work [23, 33, 34], the local porosity is smaller around two neighboring particles of different sizes than around two neighboring particles of the same size. This effect is greater for larger differences in the size of two neighbors. As skewness and polydispersity increase, both the number of small particles present and the average size discrepancy between neighboring particles increase, resulting in a larger ϕ_{rcp} .

To provide a qualitative sense of the behavior, Fig. 3 shows a 2D slice through four different 3D packings. (a) and (b) are lognormal packings, where (a) is a packing at low polydispersity and skewness and (b) is a denser packing at a higher polydispersity and skewness. Packings (c) and (d) are two binary packings with polydispersity 0.4, where (c) has a large negative skewness and (d) is denser and has a large positive skewness. As discussed above, at large δ and S , small particles can either layer around

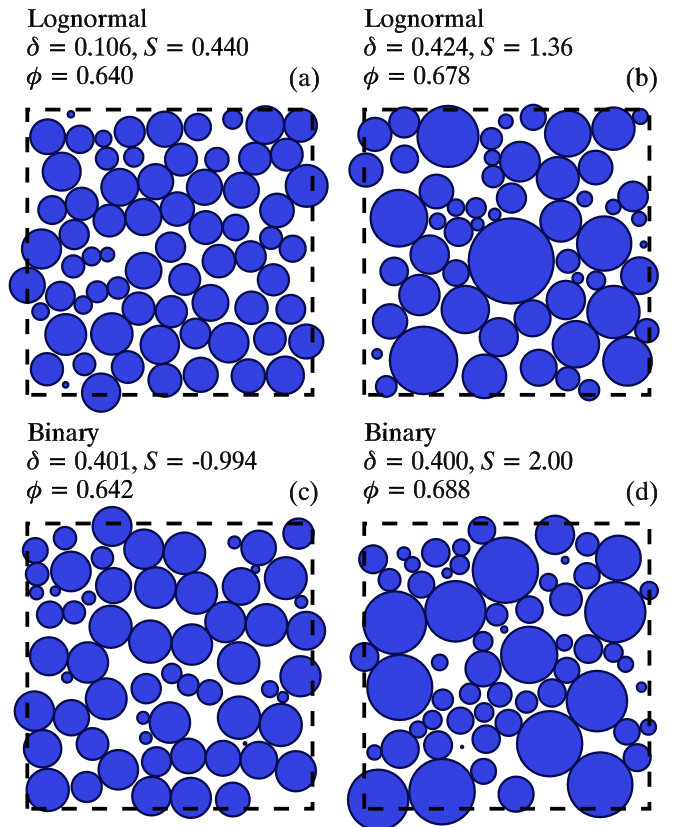


FIG. 3. (Color online). Each image represents a 2D slice through a 3D packing, and the dashed box is the boundary of the periodic packing. The volume fraction for each packing shown is close to the extrapolated ϕ_{rcp} . Also, the area fraction of each 2D slice is the same as the volume fraction of the 3D packing they represent.

larger particles and/or fit in the voids between bigger particles. In Fig. 3(b) and (d) we see evidence of small particles sitting in the void areas between big particles. In Fig. 3(a) and (c), where the skewness is lower, we see less evidence of this. These observations are consistent with the results of Fig. 2.

Since ϕ_{rcp} is nearly determined by the two parameters δ and S , we fit all the data to a simple equation $\phi_{rcp} = \phi_{rcp}^* + c_1\delta + c_2S\delta^2$, where ϕ_{rcp}^* is the packing fraction for a monodisperse packing of spheres ($\delta = 0$ and $S = 0$) and c_1 and c_2 are empirical constants. These fit lines are shown as dashed lines in Fig. 2, and agree reasonably well with the data. We also tried fits with higher order terms in S and δ , but we found first order in S and second order in δ reasonably fit all the data well. Using our simple fit model, we find $\phi_{rcp}^* = 0.634$, $c_1 = 0.0658$, and $c_2 = 0.857$. The fit gave a value for ϕ_{rcp}^* close to the experimentally accepted value of 0.637 [1, 48].

There are slight differences in the ϕ_{rcp} values for different distribution types for the same δ and S values, seen in Fig. 2. Thus far we have focused on δ and S to characterize our distributions, and of course the distributions

differ in their higher moments. The next quantity to consider is the kurtosis K defined above, and it might be a potential additional parameter to explain the variations in Fig. 2. However, comparing packings with the same δ and S we find that the slight differences in ϕ_{rcp} have no clear dependence on K , suggesting that the kurtosis is not an important contributor to the ϕ_{rcp} . This agrees with the 1933 qualitative observations of Tickell *et al.* [41].

We note in passing that a rapid prediction of ϕ_{rcp} can be found by using the numerical algorithm of Farr and Groot [35], based on any $P(R)$ as input. All of our numerical data from explicitly generating 3D packings agree quite well with the results of their algorithm.

Our data have two significant conclusions. First, the skewness S has a significant influence on ϕ_{rcp} for distributions with a large polydispersity δ . Second, knowing δ and S can determine ϕ_{rcp} to within approximately ± 0.002 without taking into account any other details of the shape of $P(R)$.

This collapse of ϕ_{rcp} values for a given δ and S but different distribution shapes is intriguing, as presumably

the structures within the packings are different for different $P(R)$. For that matter, one can have the same ϕ_{rcp} value for different δ and S , see for example Fig. 3(a) and (c), and clearly these will have different microstructures. This might be useful for studying aspects of the jamming transition of spherical particles. Many prior results show that various properties of these systems depend on the distance to the jamming point [49–53], where the jamming point is thought to be the same as ϕ_{rcp} [15, 45, 46, 54]. One can imagine conducting experiments or simulations to compare the properties of packings near the jamming transition with different microstructures, but the same jamming point. These could be equally useful for studying the colloidal glass transition, which may be influenced by ϕ_{rcp} [51, 55–59]. Such experiments may provide further insight into the universal nature of the jamming transition and glass transition, but may also highlight subtle dependencies on the microstructure.

The work of K.W.D was supported by the National Science Foundation under Grant No. CBET-0853837, and the work of E.R.W. was supported by the National Science Foundation under Grant No. CMMI-1250235.

-
- [1] S. Torquato and F. H. Stillinger, *Rev. Mod. Phys.* **82**, 2633 (Sep. 2010)
 - [2] T. M. Truskett, S. Torquato, and P. G. Debenedetti, *Phys. Rev. E* **62**, 993 (2000)
 - [3] O. K. Rice, *J. Chem. Phys.* **12**, 1 (1944)
 - [4] J. D. Bernal and J. Mason, *Nature* **188**, 910 (1960)
 - [5] W. O. Smith, P. D. Foote, and P. F. Busang, *Phys. Rev. Lett.* **34**, 1271 (1929)
 - [6] S. F. Edwards, *Granular Matter* (Springer-Verlag, 1994)
 - [7] C. Radin, *J. Stat. Phys.* **131**, 567 (2008)
 - [8] M. Jerkins, M. Schröter, H. L. Swinney, T. J. Senden, M. Saadatfar, and T. Aste, *Phys. Rev. Lett.* **101**, 018301 (2008)
 - [9] R. Pal, *Polym. Eng. Sci.* **48**, 1250 (2008)
 - [10] G. Lois, J. Blawdziewicz, and C. S. O'Hern, *Phys. Rev. Lett.* **102**, 015702 (2009)
 - [11] R. Zallen, *Physics of Amorphous Solids* (Wiley, 1983)
 - [12] C. S. O'Hern, L. E. Silbert, A. J. Liu, and S. R. Nagel, *Phys. Rev. E* **68**, 011306 (2003)
 - [13] C. S. O'Hern, L. E. Silbert, A. J. Liu, and S. R. Nagel, *Phys. Rev. E* **70**, 043302 (2004)
 - [14] R. K. Mcgeary, *J. Am. Ceram. Soc.* **44**, 513 (1961)
 - [15] S. Torquato, T. M. Truskett, and P. G. Debenedetti, *Phys. Rev. Lett.* **84**, 2064 (2000)
 - [16] A. R. Kansal, S. Torquato, and F. H. Stillinger, *J. Chem. Phys.* **117**, 8212 (2002)
 - [17] R. Al-Raoush and M. Alsaleh, *Powder Technol.* **176**, 47 (2007)
 - [18] K. Lochmann, L. Oger, and D. Stoyan, *Solid State Sci.* **8**, 1397 (2006)
 - [19] H. J. H. Brouwers, *Phys. Rev. E* **74**, 031309 (Sep. 2006)
 - [20] T. Okubo and T. Odagaki, *J. Phys-Condens. Mat.* **16**, 6651 (2004)
 - [21] P. Richard, L. Oger, J. P. Troadec, and A. Gervois, *Euro. Phys. J. E* **6**, 295 (Dec. 2001)
 - [22] B. R. Aïm and L. P. Goff, *Powder Technol.* **1**, 281 (1967)
 - [23] H. Y. Sohn and C. Moreland, *Can. J. Chem. Eng.* **46**, 162 (1968)
 - [24] A. R. Dexter and D. W. Tanner, *Science* **238**, 31 (1972)
 - [25] W. M. Visscher and M. Bolsterli, *Nature* **239**, 504 (1972)
 - [26] D. M. E. Thies-Weesie and A. P. Philipse, *Journal of Colloid and Interface Science* **162**, 470 (1994)
 - [27] A. Donev, S. Torquato, F. H. Stillinger, and R. Connelly, *J. App. Phys.* **95**, 989 (2004)
 - [28] A. Donev, F. H. Stillinger, and S. Torquato, *Phys. Rev. Lett.* **96**, 225502 (Jun. 2006)
 - [29] T. S. Hudson and P. Harrowell, *J. Phys. Chem. B* **112**, 8139 (Jul. 2008)
 - [30] W. Schaertl and H. Sillescu, *J. Stat. Phys.* **77**, 1007 (1994)
 - [31] M. Hermes and M. Dijkstra, *Europhys. Lett.* **89**, 38005 (2010)
 - [32] M. Clusel, E. I. Corwin, A. O. N. Siemens, and J. Brujic, *Nature* **460**, 611 (2009)
 - [33] H. J. H. Brouwers, *Phys. Rev. E* **74**, 031309 (2006)
 - [34] C. C. Furnas, *Ind. Eng. Chem.* **23**, 1052 (1931)
 - [35] R. S. Farr and R. D. Groot, *J. Chem. Phys.* **131**, 244104 (2009)
 - [36] D. P. Haughey and G. S. G. Beveridge, *Can. J. Chem. Eng.* **47**, 130 (1969)
 - [37] M. Subbanna, P. C. Kapur, and Pradip, *Ceram. Int.* **28**, 401 (Jan. 2002)
 - [38] M. Suzuki and T. Oshima, *Powder Technol.* **44**, 213 (Oct. 1985)
 - [39] M. J. Powell, *Powder Technol.* **25**, 45 (Jan. 1980)
 - [40] H. D. Lewis and A. Goldman, *J. Am. Ceram. Soc.* **49**, 323 (1966)
 - [41] F. G. Tickell, O. E. Mechem, and R. C. McCurdy, *T.*

- Am. I. Min. Met. Eng. **103**, 250 (1933)
- [42] N. Xu, J. Blawdziewicz, and C. S. O'Hern, Phys. Rev. E **71**, 061306 (2005)
 - [43] W. S. Jodrey and E. M. Tory, Phys. Rev. A **32**, 2347 (1985)
 - [44] J. Tobochnik and P. M. Chapin, J. Chem. Phys. **88**, 5824 (1988)
 - [45] A. Donev, S. Torquato, F. H. Stillinger, and R. Connelly, Phys. Rev. E **70**, 043301 (2004)
 - [46] C. S. O'Hern, L. E. Silbert, A. J. Liu, and S. R. Nagel, Phys. Rev. E **70**, 043302 (2004)
 - [47] K. W. Desmond and E. R. Weeks, Phys. Rev. E **80**, 051305 (2009)
 - [48] G. D. Scott and D. M. Kilgour, J. Phys. D Appl. Phys. **2**, 863 (1969)
 - [49] W. G. Ellenbroek, E. Somfai, M. van Hecke, and W. van Saarloos, Phys. Rev. Lett. **97**, 258001 (2006)
 - [50] T. S. Majmudar, M. Sperl, S. Luding, and R. P. Behringer, Phys. Rev. Lett. **98**, 058001 (2007)
 - [51] A. J. Liu and S. R. Nagel, Condens. Matter Phys. **1**, 347 (2010)
 - [52] K. W. Desmond, P. J. Young, D. Chen, and E. R. Weeks, Soft Matter **9**, 3424 (2013)
 - [53] G. Katgert and M. van Hecke, Europhys. Lett., 34002(2010)
 - [54] C. S. O'Hern, L. E. Silbert, A. J. Liu, and S. R. Nagel, Phys. Rev. E **68**, 011306 (2003)
 - [55] L. Berthier and G. Biroli, Rev. of Mod. Phys. **83**, 587 (Jun. 2011)
 - [56] P. Chaudhuri, L. Berthier, and W. Kob, Phys. Rev. Lett. **99**, 060604 (Aug. 2007)
 - [57] G. L. Hunter and E. R. Weeks, Rep. Prog. Phys. **75**, 066501 (Jun. 2012)
 - [58] E. Marcotte, F. H. Stillinger, and S. Torquato, J. Chem. Phys. **138**, 12A508 (2013)
 - [59] Z. Zhang, N. Xu, D. T. N. Chen, P. Yunker, A. M. Alsayed, K. B. Aptowicz, P. Habdas, A. J. Liu, S. R. Nagel, and A. G. Yodh, Nature **459**, 230 (2009)